Numerical Calculation of Band Layer Design for Laser Diode

[1]Thae Nu Wah and [2]Hla Myo Tun,
[1]Department of Electronics Engineering, Technological University (Mawlamyine)
[2]Department of Electronics Engineering, Yangon Technological University

Abstract— This paper is done on the analysis of computer-based simulation design for laser diode modeling. The research is emphasized by the relation of electrical and optical properties of the band structure design. For the electrical properties, threshold current temperature dependence, light-current, external differential quantum efficiency, voltage-current, temperature dependence of emission intensity, band-gap energy versus temperature curves, and band diagram are discussed briefly. On the other hand, for the band structure design, the research is emphasized by not only the existing known materials but also the other new materials. The band diagram results are approved by the parameters of the materials such as doping concentrations, effective mass of the materials and so on. Beside the fundamental materials, the band structure also shows the other new materials such as GaAs/GaInAs , and so on. This research will help the researchers who analyze the laser diodes.

Keywords—*Gaas, Gainas, Nitride Semiconductor Laser, Quantum Well Devices*

I. INTRODUCTION

LASER diode (LD) is a semiconductor optical amplifier (SOA) that has an optical feedback. A semiconductor optical amplifier is a forward-biased heavily-doped p+-n+ junction fabricated from a direct-bandgap semiconductor material. A LD device may be any element that converts electrical into light. LDs are used for optical storage (high-dendity Blu-ray^{TM} dics), laser printing and scanning, high-resolution lithography, and future pico-projection applications [1]. Since the first demonstration of blue LDs by Nakamura and co-workers in the mid 90s, the knowledge on III-nitride materials and the crystalline quality of epitaxial layers have constantly progressed [2].

Optimization of the device design is usually done by computer simulation, and this must be based upon the physical processes

which actually occur in the devices and must use appropriate values for material parameters. The I-V characteristics of the LD devices are in good agreement with the properties of the materials used for the crystal growth. The research approves the existing system from the literature background. The current-voltage characteristics of the existing materials are mentioned, such as silicon and gallium nitride [3].

The band structures of semiconductors for p-GaAs/N-$Al_{0.3}Ga_{0.7}As$, and n-GaAs/P-$Al_{0.3}Ga_{0.7}As$ are discussed with figures. The band diagrams are designed for heterojunctions. A p-type semiconductor is in contact with an N-type band-gap semiconductor or a n-type semiconductor is in contact with the P-type semiconductor. The Fermi level will line up to be a constant across the junction under thermal equilibrium conditions without any voltage bias, when the two crystals are in contact.

II. GENERATION AND RECOMBINATION PROCESS

These generation-recombination processes can be classified as radiative or nonradiative. The radiative transitions involve the creation or annihilation of photons. The nonradiative transitions do not involve photons; they may involve the interaction with phonons or the exchange of energy and momentum with another electron or hole. The recombination rate of electrons and holes should be proportional to the product of the electron and hole concentrations

$$R_n = R_p = cnp \tag{1}$$

The generation rate may be written as

$$G_n = G_p = e \tag{2}$$

where c is a capture coefficient and e is an emission rate [4].

(a) Recombination of electron-hole pair
$R_n=R_p=cnp$

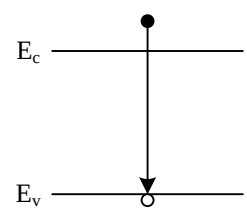

(b) Generation of electron-hole pair
$G_n=G_p=e$

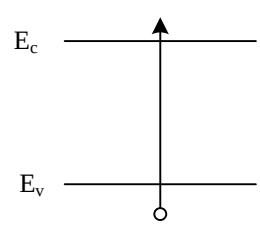

Figure 1. The energy band diagrams for (a) recombination and (b) generation of an electron-hole pair.

III. AUGER GENERATION-RECOMBINATION PROCESS

For band-to-bound state transitions, the following processes

1. Electron captures with the released energy taken by an electron or a hole. The recombination rate is given by

$$R_n = \left(c_n^n n + c_n^p p\right) n N_t \left(1 - f_t\right) \tag{3}$$

where we note that the capture coefficient c_n is SRH recombinations has been replaced by $c_n^n n + c_n^p p$, since the two possible processes for electron captures are proportional to the

concentration of the electron or hole that gains the energy released by the electron capture.

2. Electron emissions with the required energy supplied by an energetic electron or hole:

$$G_n = \left(e_n^n n + e_n^p p\right) N_t f_t \quad (4)$$

3. Hole captures with the released energy taken by an electron or a hole:

$$R_p = \left(c_p^n n + c_p^p p\right) p N_t f_t \quad (5)$$

4. Hole emissions with the required energy supplied by an energetic electron or hole:

$$G_p = \left(e_p^n n + e_p^p p\right) N_t \left(1 - f_t\right) \quad (6)$$

In this process the energy becoming available through electron-hole recombination is dissipated by the excitation of a free electron high into the conduction band, or by a hole deeply excited into the valence band [5].

IV. Current-Voltage Characteristics Of Semiconductor

The Shockley equation for a diode with cross sectional area A is

$$J_s = \frac{qD_p p_{no}}{L_p} + \frac{qD_n n_{po}}{L_n} = qn_i^2 \left(\frac{1}{N_D}\sqrt{\frac{D_p}{\tau_p}} + \frac{1}{N_A}\sqrt{\frac{D_n}{\tau_n}} \right) \quad (7)$$

where $D_{n,p}$ and $\tau_{n,p}$ are the electron and hole diffusion constants and the electron and hole minority carrier lifetimes. Under reverse bias conditions, the diode current saturates and the saturation current is given by the factor preceding the exponential function in the Shockley equation. The basic equation from the theory of semiconductors that mathematically describes the I-V characteristic of the laser diode is

$$I = A \times J_s \left[\exp\left(\frac{qV_a}{kT} \right) - 1 \right] \quad (8)$$

where, J_s = the saturation current density
I = the current
$D_{n,p}$ = electron and hole diffusion constants
$\tau_{n,p}$ = electron and hole minority carrier lifetime
$N_A = N_D$ = acceptor and donor concentration
n_i = intrinsic carrier concentration
A = area

Laser diodes have voltage-current characteristics like other diodes. A substantial current flows only above for certain critical voltage, which depends on the used material system. Above the critical voltage, the current rises rapidly with increasing voltage. A laser diode is normally not operated by applying a fixed voltage, and could also be substantially affected by the device temperature. The current-voltage (I-V) characteristic of a p-n junction was first developed by Shockley. For I-V curve of a p-n junction diode, the equation is referred by the Shockley equation. The diode current saturates and the saturation current is given by the factor preceding the exponential function in the Shockley equation, under reverse bias conditions. The current-voltage characteristics of GaAs, GaAsP, and GaInN are shown in figure 2. The threshold voltage as well as the series resistance of the diode increases as the diode is cooled. If the device were driven at a constant voltage, a large current change would result from a change in temperature.

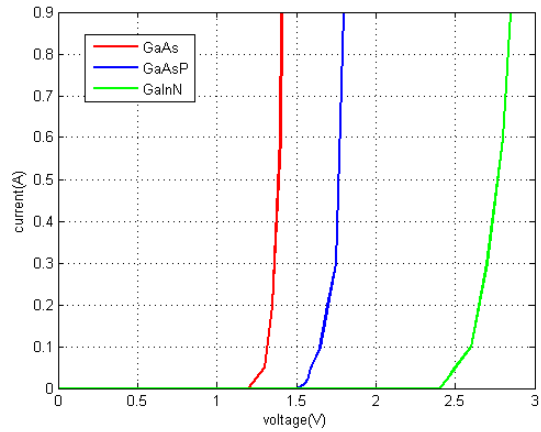

Figure 2. Current-voltage characteristics made from different semiconductors.

V. Band Diagrams Of Heterojunction

A. Band diagram of a p-GaAs/N-$Al_xGa_{1-x}As$ heterojunction

The doping concentration is $N_a = 1\times10^{18} cm^{-3}$ in the p side and $N_D = 2\times10^{17} cm^{-3}$ in the N side (x=0.3).

Assume that the density of states hole effective mass ($0 \le x \le 0.45$) is

$$m_h^*(x) = (0.50 + 0.29x) m_0 \quad (9)$$

Electron effective mass is

$$m_e^*(x) = (0.0665 + 0.083x) m_0 \quad (10)$$

The energy gap is

$$E_g(x) = (1.424 + 1.247x)(eV)$$

Dielectric constant for ($0 \le x \le 0.45$),

$$\varepsilon(x) = (13.1 - 3x)\varepsilon_0$$

x is the mole fraction of aluminium.

Table 1. Band structure parameters for GaAs/$Al_xGa_{1-x}As$

p-GaAs	N-$Al_xGa_{1-x}As$
$m_e^* = 0.0665 m_0$	$m_e^* = 0.0914 m_0$
$m_h^* = 0.50 m_0$	$m_h^* = 0.587 m_0$
$\varepsilon_p = 13.1\varepsilon_0$	$\varepsilon_N = 12.2\varepsilon_0$
$E_{gp} = 1.424 eV$	$E_{gN} = 1.798 eV$

The band edge discontinuities are

$$\Delta E_g = 1.247x$$

$$\Delta E_c = 0.67 \Delta E_g$$

$$\Delta E_v = 0.33 \Delta E_g \quad (11)$$

The concentrations are

$$N_c = 2.51\times10^{19}\left[\frac{m_e^*}{m_0}\frac{T}{300}\right]^{3/2} cm^{-3} \quad (12)$$

$$N_v = 2.51\times10^{19}\left[\frac{m_h^*}{m_0}\frac{T}{300}\right]^{3/2} cm^{-3} \quad (13)$$

$$p = N_a = N_v F_{1/2}\left[\frac{E_{vp}-F_p}{k_B T}\right] = N_v \exp\left[\frac{E_{vp}-F_p}{k_B T}\right] \quad (14)$$

$$F_p - E_{vp} = -k_B T \ln\frac{N_a}{N_v} \quad (15)$$

$$N = N_D = N_c F_{1/2}\left[\frac{F_N - E_{cN}}{k_B T}\right] = N_c \exp\left[\frac{F_N - E_{cN}}{k_B T}\right] \quad (16)$$

$$E_{cN} - F_N = -k_B T \ln\frac{N_D}{N_c} \quad (17)$$

The contact potential

$$V_0 = \frac{E_{gp} + \Delta E_c - (F_p - E_{vp}) - (E_{cN} - F_N)}{q} \quad (18)$$

The depletion widths

$$x_p = \left[\frac{2\varepsilon_p V_0}{qN_a N_D\left(N_D + \frac{\varepsilon_p}{\varepsilon_N}N_a\right)}\right]^{1/2} N_D \quad (19)$$

$$x_N = \frac{x_p}{N_D} N_a \quad (20)$$

$$x_w = x_p + x_N \quad (21)$$

The voltage drop across p-side is

$$V_{op} - V_p = \frac{qN_a}{2\varepsilon_p} x_p^2 \quad (22)$$

Also, the voltage drop across N-side is $V_{oN} - V_N = \frac{qN_D}{2\varepsilon_N} x_N^2$ (23)

The figure 3 shows that a p-type narrow-gap semiconductor in contact with an N-type wide band-gap semiconductor of heterojunction. The Fermi level will line up to be a constant across the junction under thermal equilibrium conditions without any voltage bias, when the two crystals are in contact.

As a result, the total width of the depletion region is 0.114 µm and the conduction band is very close to the Fermi level than the valence band. For p-type, the conduction band edge is 1367.6 meV.

From the design of the band diagram, the conditions of the drift current or diffusion current flowing across the heterojunction can be observed. By analyzing the energy band structure, the effect of the forward voltage or barrier voltage can be observed, especially from the differences in energy gap.

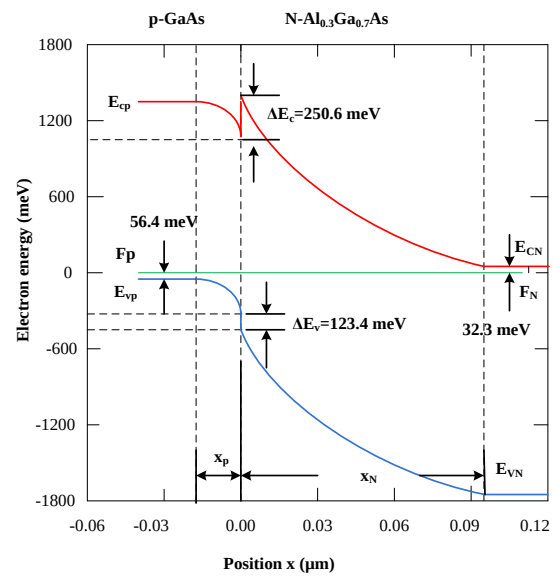

Figure 3.Band diagram of a p-GaAs/N-$Al_{0.3}Ga_{0.7}As$ heterojunction with N_a=1x10^{18} cm^{-3} in the p region and N_D=2x10^{17} cm^{-3} in the N region.

A. Band diagram of n-GaAs/P-$Al_xGa_{1-x}As$ heterojunction

The doping concentration is $N_d = 4\times10^{16} cm^{-3}$ in the p side and $N_A = 2\times10^{17} cm^{-3}$ in the N side (x=0.3).

The concentrations are as follows.

$$n = N_d = N_c F_{1/2}\left[\frac{F_n - E_{cn}}{k_B T}\right] = N_c \exp\left[\frac{F_n - E_{cn}}{k_B T}\right] \quad (24)$$

$$E_{cn} - F_n = -k_B T \ln\frac{N_d}{N_c} \quad (25)$$

$$P = N_A = N_v F_{1/2}\left[\frac{E_{vP} - F_P}{k_B T}\right] = N_v \exp\left[\frac{E_{vP} - F_P}{k_B T}\right] \quad (26)$$

$$F_P - E_{vP} = -k_B T \ln\frac{N_A}{N_v} \quad (27)$$

The contact potential

$$V_0 = \frac{E_{GP} - \Delta E_c - (E_{cn} - F_n) - (F_P - E_{vP})}{q} \quad (28)$$

The depletion widths

$$x_n = \left[\frac{2\varepsilon_n V_0}{qN_d N_A \left(N_A + \frac{\varepsilon_n}{\varepsilon_P} N_d \right)} \right]^{1/2} N_A \quad (29)$$

$$x_P = \frac{x_n}{N_A} N_d \quad (30)$$

The voltage drop across the n-side

$$V_{on} - V_n = \frac{qN_d}{2\varepsilon_n} x_n^2 \quad (31)$$

The voltage drop across the P-side

$$V_{oP} - V_P = \frac{qN_A}{2\varepsilon_P} x_P^2 \quad (32)$$

The band structure of semiconductor n-P heterojunction is shown in figure 4. The step by step procedure to find the band diagram of n-P heterojunction is similar to that of the p-N heterojunction. The figure reveals that the wide-gap semiconductor is doped P-type and the narrow gap semiconductor is doped n-type. When the heterojunction is formed, a space charge region will exist due to the diffusion or redistribution of free carriers at thermal equilibrium. As a result, the total width of the depletion region is 0.24 µm and the conduction band is very close to the Fermi level than the valence band.

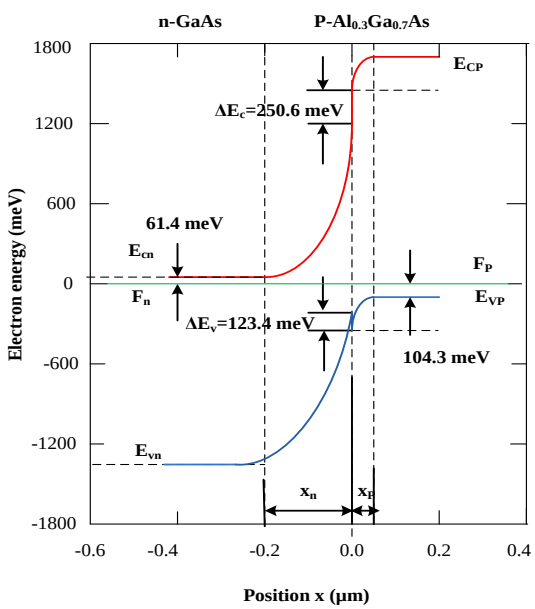

Figure 4. Band diagram of an unbiased n-GaAs/P-$Al_{0.3}Ga_{0.7}As$ heterojunction with $N_d=4x10^{16}$ cm^{-3} in the n region and $N_A=2x10^{17}cm^{-3}$ in the P region.

CONCLUSION

Analyzing the mathematical equations and changing the semiconductor materials will give the new characteristics and properties with the high accuracy and high performance of laser diode. The current-voltage characteristics of materials, the comparison of optical emission spectra, the energy band-gap structure have been discussed. The band-gap energy as a function of temperature has also been described. Therefore, the development of the device with the help of computerized analysis will be provided the physical properties and characteristics of the unknown materials that are used in LDs. According to this research, the best design for laser diode can be developed.

REFERENCES

[1] U. Strauss, S. Brüninghoff, M. Schillgalies, C. Vierheilig, N. Gmeinwieser, V. Kümmler, G. Brüderl, S. Lutgen, A. Avramescu, D. Queren, D. Dini, C. Eichler, and A. Lell: Proc. SPIE 6894 (2008) 689417.

[2] S. Nakamura, M. Senoh, S. Nagahama, N. Iwasa, T. Yamada, T. Matsushita, H. Kiyoku, and Y. Sugimoto: Jpn.J. Appl. Phys. 35 (1996) L74.

[3] D. P. Bour, R. S. Geels, D. W. Treat, T. L. Paoli, F. Ponce, R. L. Thornton, B. S. Krusor, R. D. Briggins, and D. F. Welch, "Strained layer GaInP/AlGaInP heterostructures and quantum well laser diodes," *IEEE J. Quantum Electron.*, vol. 30, pp. 593–606, Feb. 1994.

[4] D. P. Bour, D. W. Treat, R. L. Thornton, R. S. Geels, and D. F. Welch, "Drift leakage current in AlGaInP quantum well lasers," *IEEE J. Quantum Electron.*, vol. 29, pp. 1337–1343, May 1993.

[5] P. M. Smowton and P. Blood, "GaInP-AlGaInP 670 nm quantum well lasers for high temperature operation," *IEEE J. Quantum Electron.*, vol. 31, pp. 2159–2164, Dec. 1995.

[6] D. L. Foulger, P. M. Smowton, P. Blood, and P. W. Mawby, "Self-consistent simulation of AlGaInP/GaInP visible lasers," *Proc. Inst. Elect. Eng.*, pt. J, vol. 144, pp. 23–29, Feb. 1997.

[7] Claire F. Gmachl, David P. Bour: "Novel In-Plane Semiconductor Lasers III", Proceedings of SPIE Vol.5365, doi: 10.1117/12.528329.

[8] H. C. Casey, Jr., "Temperature dependence of threshold current density on InP-Ga0.28In0.72As0.6P0.4 (1.3 µm) double heterostructure lasers," J.Appl. Phys., vol. 56, no. 7, pp. 1959-1964, 1984.

[9] R. Binder, P. Blood & M. Osinski: "Physics and Simulation of Optoelectronic Devices VIII", SPIE Proc. 3944, 2000.

[10] S. M. Sze, "Physics of Semiconductor Devices", 2nd ed., Wiley, New York, 1981, Ch. 12-14.

[11] H. Baltes, and D. Liepmann : "Laser diode Microsystems", pp. 55-60, SPIN: 10857158.

[12] N. Tansu and L. J. Mawst, "Low-threshold-current strain-compensated InGaAs(N)-GaAsP-InGaP (λ = 1.19-1.3 µm) quantum well diode lasers," IEEE Photon. Technol.Lett., vol. 14, pp. 444-446, Apr. 2002.

[13] Zhores Alferov, "Double heterostructure lasers": early days and future perspectives, IEEE Journal on Selected Topics in Quantum Electronics, Vol. 6, pp. 832-840, Nov/Dec 20.